Adenosine 5′-O-(3-thio)triphosphate (ATPγS) is a substrate for the nucleotide hydrolysis and RNA unwinding activities of eukaryotic translation initiation factor eIF4A

MATTHEW L. PECK and DANIEL HERSCHLAG
Department of Biochemistry, Stanford University, Stanford, California 94305-5307, USA

ABSTRACT

Whereas ATPγS is often considered a nonhydrolyzable substrate for ATPases, we present evidence that ATPγS is a good substrate for the RNA-stimulated nucleotide hydrolysis and RNA unwinding activities of eIF4A. In the presence of saturating single-stranded poly(U) RNA, eIF4A hydrolyzes ATPγS·Mg and ATP·Mg with similar steady-state parameters ($K_M^{NTP\cdot Mg}$ = 66 and 58 μM and k_{cat} = 1.0 and 0.97 min^{-1}, respectively). ATPγS·Mg also supports catalysis of RNA unwinding within 10-fold of the rate supported by ATP·Mg. The identical steady-state rate parameters, in comparison with the expected difference in the intrinsic rate of hydrolysis for ATP and ATPγS, suggest a nonchemical rate-limiting step for nucleotide hydrolysis. These results raise caution concerning the assumption that ATPγS is a nonhydrolyzable ATP analog and underscore the utility of thio-substituted NTPs as mechanistic probes.

Keywords: ATPγS; DEAD box protein; DExD/H box protein; RNA helicase; ATPase; unwindase; thio-effect

INTRODUCTION

To initiate the translation of a typical mRNA, the 43S ribosomal complex is thought to bind to an mRNA near its 5′-cap and then scan 5′ to 3′ along the untranslated region (UTR) in search of the first initiator AUG codon (Kozak 1992; Merrick and Hershey 1996). This overall process requires ATP and the ATPase activity of eukaryotic initiation factor 4A (eIF4A; Trachsel et al. 1977; Benne and Hershey 1978; Linder and Slonimski 1989; Blum et al. 1992).

RNA structure in the 5′-UTR can inhibit translation initiation, and several lines of evidence suggest that part of biological role of eIF4A may be to remove RNA structure (Pelletier and Sonenberg 1985; Kozak 1986; Svitkin et al. 2001). The ATPase activity of eIF4A is stimulated by single-stranded RNA (ssRNA; Grifo et al. 1984; Abramson et al. 1987). In vitro, eIF4A performs ATP-dependent unwinding of RNA and RNA·DNA duplexes (Rogers et al. 1999, 2001a). This unwinding activity is enhanced by initiation factors eIF4B, eIF4H, and eIF4G (Abramson et al. 1988; Rozen et al. 1990; Richter-Cook et al. 1998; Rogers et al. 1999, 2001b). eIF4A possesses short motifs of amino acid sequence that are the signature of the so-called helicase family of proteins (Gorbalenya and Koonin 1993). Nevertheless, it remains unclear if all subgroups of the helicase family, such as DExD/H box proteins, perform bona fide nucleic acid unwinding in vivo (Staley and Guthrie 1998; Lorsch and Herschlag 1998a; Tanner and Linder 2001; Caruthers and McKay 2002; Singleton and Wigley 2002). To understand the diversity of function within this protein family and to more fully define the role of eIF4A in translation, it is important to mechanistically dissect reactions of helicase family members and to identify conserved and distinguishing biochemical and structural features of these enzymes.

We have assessed the effect of adenosine 5′-O-(3-thio) triphosphate (ATPγS), in which one of the nonbridging oxygens of the γ-phosphoryl group is replaced by sulfur, on the activities of eIF4A. This sulfur substitution has deleterious effects on the activity of many NTPases, hydrolases, and phosphorylases (Eckstein 1983, 1985; Zhang et al. 1999). The effects presumably arise from the distinct steric and electronic properties of sulfur compared with oxygen

Reprint requests to: Daniel Herschlag, Department of Biochemistry, B400 Beckman Center, Stanford University, Stanford, CA 94305-5307, USA; e-mail: herschla@cmgm.stanford.edu; fax: (650) 723-6783.

Abbreviations: AMP-PNP, adenylyl imidodiphosphate; ATPγS, adenosine 5′-O-(3-thio)triphosphate; dsRNA, double-stranded (duplex) RNA; eIF, eukaryotic translation initiation factor; SF1, Helicase Super-family 1; SF2, Helicase Super-family 2; ssRNA, single-stranded RNA; UTR, untranslated region.

Article and publication are at http://www.rnajournal.org/cgi/doi/10.1261/rna.2103703.

(Cohn 1982; Eckstein 1985; Frey and Sammons 1985). To our surprise, we found that ATPγS·Mg is hydrolyzed by eIF4A with the same k_{cat} as ATP·Mg and supports RNA unwinding by eIF4A and eIF4B.

RESULTS

RNA-dependent Hydrolysis of ATPγS·Mg by eIF4A

Nucleotide hydrolysis was monitored to determine if ATPγS·Mg is accepted as a substrate by eIF4A. Rate constants were determined by measuring the formation of thiophosphate product at various times by using a radioactivity-based assay (Materials and Methods). As observed for ATP·Mg hydrolysis (Grifo et al. 1984; Abramson et al. 1987), ATPγS·Mg hydrolysis by eIF4A is stimulated by single-stranded poly(U) RNA (Fig. 1A).

To compare the steady-state kinetic parameters for the hydrolysis of ATPγS·Mg and ATP·Mg, hydrolysis activity was measured over a series of concentrations of ATPγS·Mg or ATP·Mg in the presence of saturating poly(U) RNA (Fig. 1B). These dependencies exhibit saturation behavior yielding values of $K_M^{NTP\cdot Mg}$ and k_{cat} for ATPγS·Mg and ATP·Mg that are the same within experimental error (66 ± 9 and 58 ± 11 μM and 1.01 ± 0.04 and 0.97 ± 0.06 min^{-1}, respectively). Thus, replacing a nonbridging oxygen at the γ-phosphoryl position of the nucleotide with sulfur has no effect on the rate-limiting step for nucleotide hydrolysis.

ATPγS hydrolysis is also observed when $MgCl_2$ is replaced by low concentrations of $CdCl_2$ (data not shown). Changing the bound metal ion in the active site presumably repositions the sulfur group because Mg^{2+} ions strongly prefer to coordinate with oxygen rather than with sulfur, and Cd^{2+} ions prefer to coordinate with sulfur rather than with oxygen (Pecoraro et al. 1984). Thus, it appears that ATPγS hydrolysis can occur with the sulfur group located in different positions of the active site of eIF4A. Inhibition of the ATP and ATPγS reactions by high concentrations of Cd^{2+} ions precluded quantitative comparisons of the reactions with Mg^{2+} and Cd^{2+} ions.

To more fully compare the ATPγS·Mg and ATP·Mg hydrolysis reactions, we established minimal kinetic and thermodynamic frameworks for each reaction (Fig. 2). As previously observed (Lorsch and Herschlag 1998a), ATP·Mg and poly(U) RNA binding is cooperative, as $K_M^{NTP\cdot Mg}$ decreases threefold when eIF4A is saturated with ATP·Mg (E·ATP). Control experiments indicate that the two- to eightfold differences from previously reported K_M values (Lorsch and Herschlag 1998a; Peck and Herschlag 1999) are due to differences in the buffer conditions (data not shown). In contrast, ATPγS·Mg and poly(U) RNA binding appears to be slightly anti-cooperative, with $K_M^{NTP\cdot Mg}$ increasing twofold when eIF4A is saturated with ATPγS·Mg (E·ATPγS). This result suggests that the sulfur substitution perturbs ground-state communication between the ATP and RNA binding sites.

RNA unwinding in the presence of ATPγS·Mg

The efficient hydrolysis of ATPγS·Mg by eIF4A encouraged us to determine if ATPγS·Mg could support the RNA unwinding activity of eIF4A. Even with efficient hydrolysis, the sulfur substitution on the γ-phosphoryl group could have deleterious effects on conformational changes required for RNA unwinding.

Unwinding reactions were assayed in the presence of trace amounts of a radiolabeled RNA duplex and excess

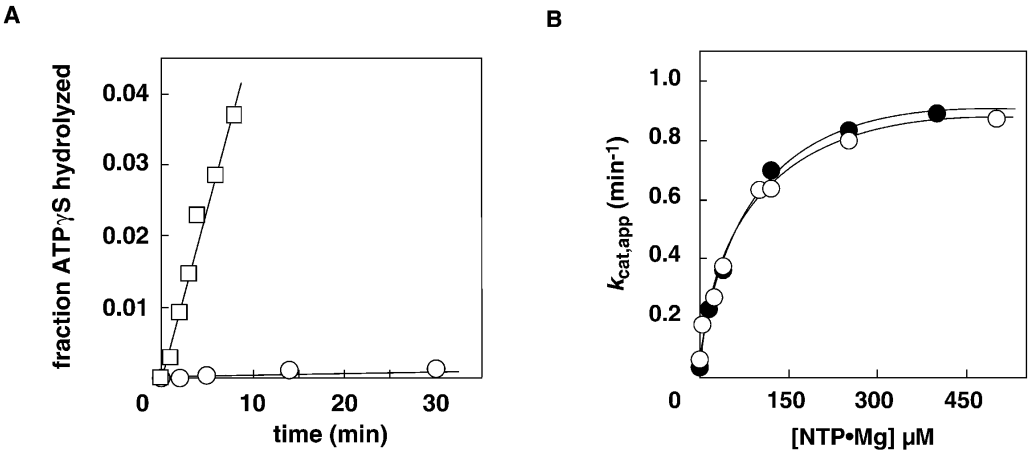

FIGURE 1. eIF4A catalyzes RNA-dependent ATPγS·Mg hydrolysis. (*A*) Fraction ATPγS·Mg hydrolyzed versus time in reactions containing 1 μM ATPγS·Mg, 0.25 μM eIF4A, and either no added RNA (○) or 25 μM poly(U) RNA (□). The slopes of linear fits yield observed rate constants ($k_{obs,hyd}$) of 2.6×10^{-5} and 4.8×10^{-3} min^{-1}, respectively. (*B*) Dependence of hydrolysis activity ($k_{cat,app}$) on the concentration of ATPγS·Mg (●) or ATP·Mg (○) in the presence of saturating poly(U) RNA (200 μM) and 0.25 μM eIF4A. The curves represent fits to the Michaelis-Menten model, yielding $K_M^{ATP\gamma S\cdot Mg} = 66 \pm 9$ μM, $K_M^{ATP\cdot Mg} = 58 \pm 11$ μM, $k_{cat}^{ATP\gamma S\cdot Mg} = 1.0 \pm 0.1$ and $k_{cat}^{ATP\cdot Mg} = 0.97 \pm 0.06$ min^{-1}.

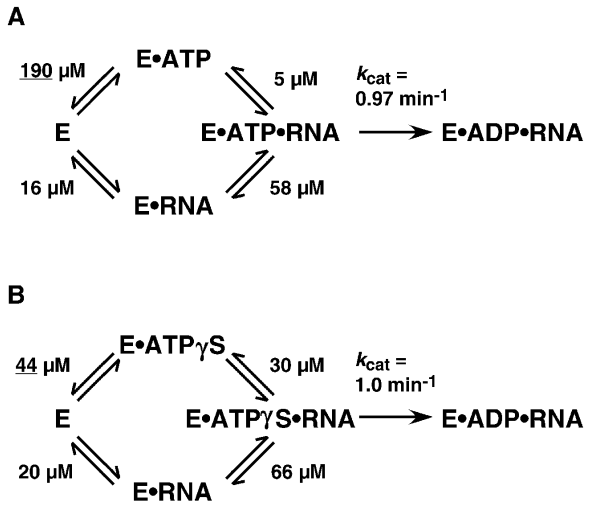

FIGURE 2. Minimal kinetic and thermodynamic schemes for the eIF4A-catalyzed hydrolysis of ATP·Mg (*A*) and ATPγS·Mg (*B*). K_M values were determined in independent experiments, except underlined values that were calculated based on the thermodynamic cycles shown. K_M values are believed to directly reflect the equilibrium dissociation constants for RNA and nucleotide binding (Lorsch and Herschlag 1998a). Unbound ligands are not depicted for clarity. E·ADP·inorganic phosphate (or inorganic thiophosphate)·RNA complexes are not depicted because is appears that eIF4A has low affinity for inorganic phosphate, and this ternary complex has not been observed (Lorsch and Herschlag 1998a).

concentrations of eIF4A and eIF4B (Fig. 3A). Nondenaturing electrophoresis was used to separate radioactively labeled ssRNA product from the duplex RNA substrate (Fig. 3B; Materials and Methods). The fraction of ssRNA formed at various times could be fit to a first-order kinetic model to yield an observed rate constant for unwinding ($k_{obs,unw}$; Fig. 3C). As shown in Figure 3C, ATPγS·Mg catalyzes unwinding rates that are at least 100-fold above those observed in the absence of nucleotide. Previously, it was reported that RNA unwinding does not occur in the presence of ATPγS·Mg (Pause et al. 1993). However, the level of activity observed here may have been too low to be detected in the previous study and ATPγS can be contaminated with ADP, which gives strong product inhibition of eIF4A reactions (Lorsch and Herschlag 1998a).

To compare the rate of unwinding with ATPγS·Mg and ATP·Mg, the dependence of $k_{obs,unw}$ on ATPγS·Mg or ATP·Mg concentration was measured in the presence of subsaturating eIF4A and saturating eIF4B (Fig. 3D). These dependencies were fit to a rapid pre-equilibrium binding model (Equation 1), yielding $K_{1/2}^{NTP\cdot Mg}$ values of 52 ± 8 and 96 ± 18 μM for ATPγS·Mg and ATP·Mg, respectively. These $K_{1/2}$ values are similar to the K_M values for NTP hydrolysis with subsaturating RNA (35 and 200 μM; Fig. 2), as expected if the NTP binding site of eIF4A is required for the unwinding reaction. Nevertheless, $k_{obs,unw}$ with saturating ATPγS·Mg ($k_{unw,max}/K_{1/2}^{eIF4A}$) was 20-fold slower than the rate-constant with saturating ATP·Mg.

$$E + NTP + dsRNA \overset{K_{1/2}^{NTP}}{\rightleftharpoons} E\cdot NTP + dsRNA \xrightarrow{(k_{unw,max}/K_{1/2}^{eIF4A})} \text{products} \quad (1)$$

$$E\cdot NTP + dsRNA \overset{K_{1/2}^{eIF4A}}{\rightleftharpoons} E\cdot NTP \cdot dsRNA \xrightarrow{k_{unw,max}} \text{products} \quad (2)$$

Because eIF4A is subsaturating, the 20-fold slower reaction with ATPγS·Mg could be due to relatively weak RNA binding by the E·ATPγS complex ($K_{1/2}^{eIF4A}$; Equation 2), as observed in the hydrolysis reaction (Fig. 2), or a slower maximal rate-constant ($k_{unw,max}$; Equation 2). To distinguish these effects, the dependence of unwinding activity on eIF4A concentration was measured in the presence of saturating ATPγS·Mg or ATP·Mg (Fig. 4). The dependence with ATPγS·Mg is linear up to 30 μM eIF4A ($K_{1/2}^{eIF4A} > 30$ μM), whereas the dependence with ATP·Mg shows significant saturation behavior at 25 μM eIF4A ($K_{1/2}^{eIF4A} \sim 15$ μM). The more than twofold difference in $K_{1/2}^{eIF4A}$ suggests that at least twofold of the 20-fold difference in ($k_{unw,max}/K_{1/2}^{eIF4A}$) arises from weaker binding of RNA by E·ATPγS than by E·ATP. This result is consistent with the approximately sixfold weaker binding of ssRNA to E·ATPγS than to E·ATP observed in the nucleotide hydrolysis assays (Fig. 2). Thus, the rate constant for RNA unwinding ($k_{obs,max}$) by the ternary complex with ATPγS·Mg present is within 10-fold of the rate constant with ATP·Mg present.

Surprisingly, the maximal observed rate constant for RNA unwinding (>8 min^{-1}; Fig. 4) is about an order of magnitude larger than k_{cat} for ATP hydrolysis (1 min^{-1}; Fig. 1B). A faster rate constant for unwinding was unexpected because ATP hydrolysis is presumably required for RNA unwinding. There are several explanations for this observation that cannot yet be distinguished. First, eIF4B or duplex RNA present in the unwinding reactions may stimulate ATP hydrolysis. eIF4B purified from rabbit reticulocytes and wheat germ has been shown to stimulate RNA and ATP binding in eIF4A-dependent ATP hydrolysis assays (Abramson et al. 1988; Browning et al. 1989; Bi et al. 2000). However, recombinant mammalian eIF4B does not appear to have an effect on substrate binding or k_{cat} in ATP hydrolysis assays (Lorsch and Herschlag 1998a; data not shown). The RNA duplex used in the unwinding assay, hairpin RNA duplexes, or hairpin RNAs with a single-stranded overhang did not stimulate ATP hydrolysis (Lorsch and Herschlag 1998a; data not shown). Reactions including both recombinant eIF4B and structured RNAs also did not produce increased rates of ATP hydrolysis (data not shown). Second, ~90% of the enzyme could be inactive for ssRNA-dependent hydrolysis but active in unwinding the duplex RNA. The observation that K_M^{RNA} for hydrolysis (5 μM; Fig. 2) is similar to $K_{1/2}^{eIF4A}$for RNA unwinding (15 μM; Fig. 4) does not support this explanation. Third, differences

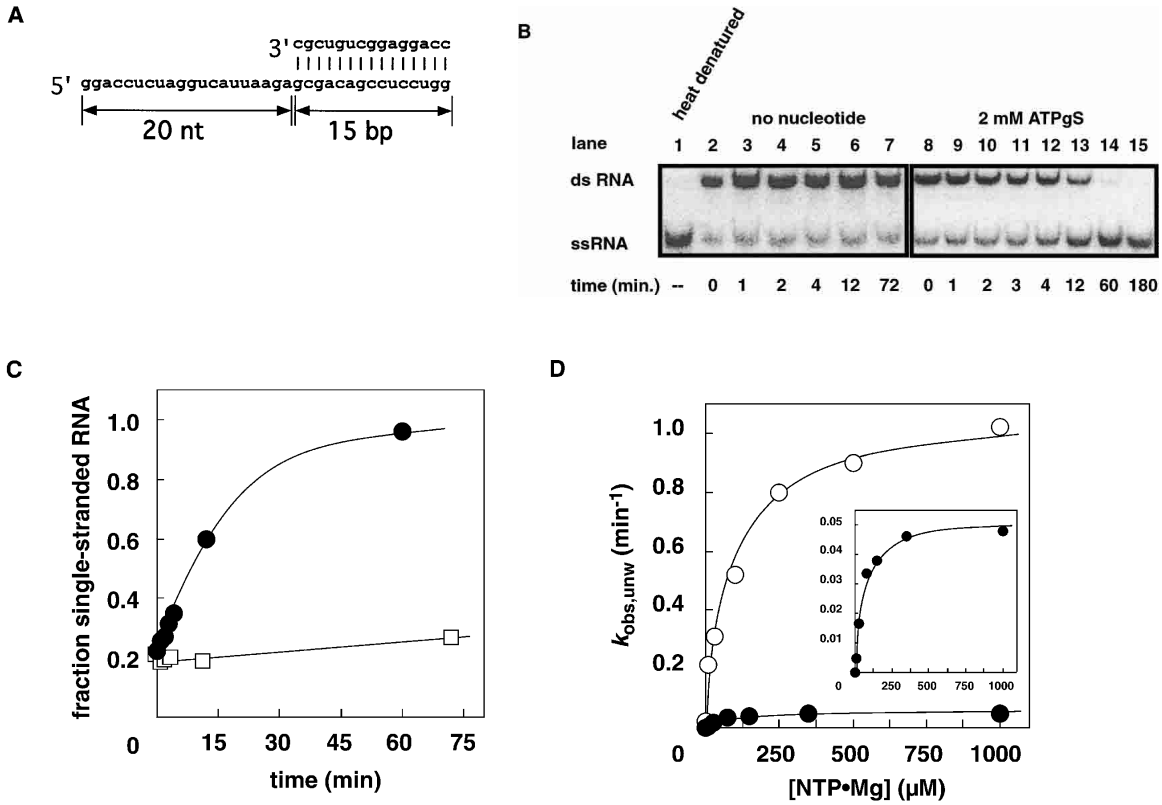

FIGURE 3. ATPγS·Mg and ATP·Mg catalyze eIF4A-dependent unwinding of RNA. (*A*) The duplex RNA substrate used in the unwinding assay. (*B*) Separation of radiolabeled single-stranded RNA product (ssRNA) from radiolabeled duplex RNA substrate (dsRNA) by nondenaturing gel electrophoresis. RNA was incubated for 5 min at 90°C (lane *1*), or with 1 μM eIF4A (subsaturating) and 0.75 μM eIF4B (saturating) for indicated times in the absence (lanes *2–7*) or presence (lanes *8–15*) of 2 mM ATPγS·Mg. (*C*) Quantification of the reactions shown in *B*. Fraction RNA unwound versus time in reactions containing no nucleotide (□) or 2 mM ATPγS·Mg (●), yielding observed rate constants ($k_{obs,unw}$) of 6.0×10^{-4} and 5.6×10^{-2} min^{-1}, respectively. (*D*) Dependence of unwinding rate ($k_{obs,unw}$) on the concentration of ATP·Mg (○) and ATPγS·Mg (●) in the presence of 1 μM eIF4A and 0.75 μM eIF4B. The curves represent fits to the Michaelis-Menten model, yielding $K_{1/2}^{ATP\cdot Mg} = 52 \pm 8$ μM, $K_{1/2}^{ATP\gamma S\cdot Mg} = 96 \pm 18$ μM and maximum $k_{obs,unw}$ values of 1.1 ± 0.2 min^{-1} and 0.052 ± 0.08 min^{-1}, respectively.

in the RNA concentrations in the unwinding assay (RNA substoichiometric to enzyme) and hydrolysis assay (RNA superstoichiometric to enzyme) could result in the formation of a multimeric eIF4A complex that possesses stimulated ATPase activity in unwinding, but not hydrolysis, reactions. However, control hydrolysis reactions containing eIF4A at concentrations up to 20-fold higher than ssRNA or duplex RNA concentrations did not show any indication of stimulated ATPase activity or multimerization (data not shown). Fourth, eIF4A may be able to catalyze a single round of RNA unwinding before the rate-limiting step for ATP hydrolysis. Another possibility is that partially unwound RNA complexes produced in the absence of ATP hydrolysis become fully dissociated when they are released by eIF4A upon quenching with SDS. In this situation, unwinding would appear to occur faster than ATP hydrolysis.

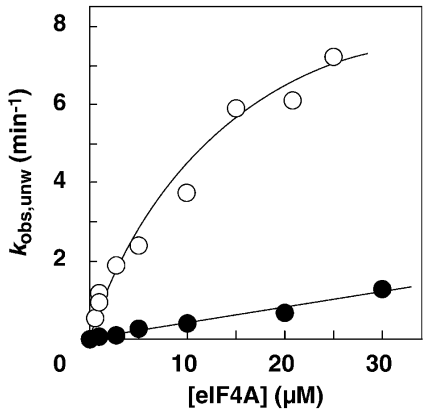

FIGURE 4. Dependence of the unwinding activity ($k_{obs,unw}$) on the concentration of eIF4A. Unwinding reactions contained 0.75 μM eIF4B, varying concentrations of eIF4A and 500 μM ATPγS·Mg (●) or ATP·Mg (○). The solid curves through the data represent a fit to a line (●), yielding a slope of 4.1×10^{-2} μM^{-1}min^{-1}, or a fit to the Michaelis-Menten model (○), yielding a $K_{1/2}$ for eIF4A of 15 μM and a maximal rate constant of 12 min^{-1} ($k_{cat}/K_{1/2}^{eIF4A} = 0.8$ μM^{-1}min^{-1}).

DISCUSSION

Surprisingly, ATPγS·Mg is comparable to ATP·Mg as a substrate for the nucleotide hydrolysis and RNA unwinding

activities of mammalian eIF4A. k_{cat} for ATPγS·Mg and ATP·Mg hydrolysis are the same within error, and the maximal rate constant for RNA unwinding with ATPγS·Mg is within 10-fold of the activity supported by ATP·Mg. These results underscore that caution should be exercised when considering ATPγS as a nonhydrolyzable analog of ATP. Our results also serve as an example of how thio-substituted ATP analogs can be used as mechanistic probes for obtaining structural and biochemical information about an enzyme.

The simplest model for the similar rates of ATP·Mg and ATPγS·Mg hydrolysis includes the following two features. First, the sulfur group appears to adopt a position in the active site where there is normally no interaction with the enzyme and no disruptive interactions are introduced. Alternatively, the sulfur reproduces interactions that were provided by the replaced oxygen, but differences in the size, bond length, electronegativity, and hydrogen bonding potential of sulfur and oxygen would require substantial plasticity within such an active-site (Cohn 1982; Eckstein 1985; Frey and Sammons 1985; Zhang et al. 1999). Second, the similar k_{cat} values for ATPγS·Mg and ATP·Mg hydrolysis are consistent with a nonchemical step being rate-limiting for hydrolysis. Based solely on simple chemical considerations, it is expected that ATPγS would be hydrolyzed *faster* than ATP. Although the rates of nonenzymatic hydrolysis of ATPγS and ATP have not been directly compared, studies of *p*-nitrophenylphosphorothioate and *p*-nitrophenylphosphate dianions, which have a similar leaving group pK_a as ATPγS and ATP, indicate that thio-substitution increases hydrolysis rates 10- to 13-fold (Domanico et al. 1986; Hollfelder and Herschlag 1995; Catrina and Hengge 1999). Based on this comparison, our results, and previous observations that eIF4A binds substrates weakly (Lorsch and Herschlag 1998a), we suggest that the rate-limiting step for ATP hydrolysis by eIF4A may not be the chemical step but may be, instead, a conformational change that occurs after substrate binding.

In contrast to our finding with eIF4A, the activities of many, but not all, ATP-using and phosphoryl transfer enzymes are greatly compromised by thio-substitution of ATP (Eckstein 1983, 1985; Zhang et al. 1999). Indeed, ATPγS has different effects on different members of the helicase superfamily. UvrD, a DNA helicase that belongs to Helicase Super-family 1 (SF1) group of the helicase superfamily, does not appear to unwind DNA in the presence of ATPγS (Matson and George 1987; Wong and Lohman 1992). RecA, a DNA-dependent ATPase that possesses a nucleotide active site that is highly similar to SF1 helicases (Korolev et al. 1998), hydrolyzes ATPγS >1000-fold more slowly than ATP (Stole and Bryant 1997). In contrast, Prp22, a member of the SF2 helicase superfamily (like eIF4A), can use ATPγS to support an RNA unwinding activity that is significantly above the level supported by adenylyl imidodiphosphate (AMP-PNP; another ATP analog) and within 20-fold of the level supported by ATP (Wagner et al. 1998). As more biochemical information about other helicase superfamily proteins is obtained, it will be of interest to see if the biochemical effects of ATPγS, and other NTPs, correlate with the structure and sequence motifs of different subgroups within the superfamily.

One might anticipate that enzymes that couple a cycle of NTP hydrolysis to perform work via conformational transitions would be particularly sensitive to substitutions of the γ-phosphoryl group. This is because contacts between the protein and the γ-phosphoryl group of the nucleotide are thought to be crucial for mediating conformational changes used by many NTPases, including DNA helicases, cytoskeletal motor proteins, and G proteins, to perform work (Smith and Rayment 1996; Velankar et al. 1999; Vale and Milligan 2000). It has been suggested that the γ-phosphoryl group could mediate analogous conformational changes in eIF4A (Lorsch and Herschlag 1998b). ssRNA binding is cooperative with ATP binding, but not ADP binding, and limited proteolysis and cross-linking results indicate that the enzyme adopts different conformations when bound to ADP and ATP analogs (Lorsch and Herschlag 1998b). Further, our results demonstrate a sixfold effect of ATPγS (relative to ATP) on binding of poly(U) RNA and possibly an effect of up to 10-fold on the rate constant for unwinding (Figs. 2, 4). It is important to recognize that thio-substitution of ATP does exert some mild effects on eIF4A activity and, presumably, structure.

In future investigations, ATPγS, and possibly other thio-substituted ATP analogs, may serve as powerful mechanistic probes to help further elucidate rate-limiting steps and the role of conformational changes in performing work. For example, ATP analogs could be of aid in further investigating the chemical step for ATP hydrolysis by eIF4A. Other initiation factors, such as eIF4G, eIF4B, and eIF4H, that presumably interact with eIF4A during translation initiation may enhance the hydrolysis, unwinding, and, potentially, scanning efficiency of eIF4A (Abramson et al. 1988; Rozen et al. 1990; Richter-Cook et al. 1998; Rogers et al. 1999, 2001b; M. Peck and D. Herschlag, unpublished results). Thus, it would also be of interest to see if the relatively mild effects of ATPγS on eIF4A activities are exacerbated in more fully reconstituted and efficient systems that contain these additional factors. Finally, it is possible that the ability of eIF4A to use ATPγS efficiently may provide an opportunity to isolate the role of eIF4A from the roles that other ATPases play in translation assays using reconstituted systems and extracts.

MATERIALS AND METHODS

Proteins

Mouse eIF4AI was overexpressed in *Escherichia coli* and purified as previously described (Peck and Herschlag 1999). The eIF4A storage buffer was 20 mM Tris-Cl (pH 7.4), 0.1 mM EDTA, 2 mM

dithiothreitol, 10% glycerol, and 80 mM potassium acetate. eIF4A was kept at −80°C for long-term storage. Aliquots at 4°C maintained full activity for at least 2 months. Overexpression and purification of human eIF4B in *E. coli* was as previously described (Lorsch and Herschlag 1998a). eIF4B was stored in 20 mM Tris-Cl (pH 7.4), 0.1 mM EDTA, 2 mM dithiothreitol, 10% glycerol, and 100 mM KCl at −80°C.

Nucleotides

ATP was from Calbiochem, ADP was from Sigma, and ATPγS was from Boehringer-Mannheim. These nucleotides were titrated to pH 7.0 with KOH and were always used in stoichiometric amounts with $MgCl_2$ or $CdCl_2$ (hereafter ATP·Mg, etc.). [γ-^{32}P]-ATP and [^{35}S]-ATPγS were purchased from ICN and purified by gel electrophoresis (Lorsch and Herschlag 1998a).

Nucleotide hydrolysis assay

Hydrolysis assays were performed by using trace amounts of radiolabeled nucleotides (<25 nM) and varying concentrations of unlabeled nucleotides in excess of protein concentration. Reactions were typically carried out at 25°C in 25 mM MES-KOH, 12 mM Tris-Cl, 2.5 mM $MgCl_2$, 2.2 mM dithiothreitol, 6% glycerol, 60 μM EDTA, 34 mM potassium acetate, and 30 mM KCl at pH 6.0 (which includes contributions from protein storage buffers). $MgCl_2$ was omitted in reactions containing $CdCl_2$. Poly(U) RNA (Pharmacia) was the ssRNA cofactor for hydrolysis reactions and its concentration is reported in 20-mer equivalents (i.e., the concentration of RNA nucleotide divided by 20) to facilitate comparisons with previous studies.

Aliquots from reactions were collected, and products were separated using poly(ethylenenimine) cellulose chromatography or nondenaturing 20% polyacrylamide gel electrophoresis (for all ATPγS reactions). PhosphoImager quantification was used to obtain observed rate constants as previously described (Peck and Herschlag 1999). The product of [^{35}S]-ATPγS hydrolysis by eIF4A migrates with a slightly faster mobility than inorganic phosphate on 20% nondenaturing gels and is presumed to be ^{35}S-thiophosphate. To avoid product inhibition by ADP (K_I^{ADP} = 2 and 10 μM with subsaturating and saturating poly[U], respectively; Lorsch and Herschlag 1998a; data not shown), initial reactions (<10% completion) were followed, and these reactions were found to be linear (e.g., Fig. 1A). K_M and k_{cat} values were obtained by fitting the dependence of the hydrolysis rate on the concentration of a reaction component to the standard Michaelis-Menten model (Segel 1993) by using KaleidaGraph Software (Synergy).

Unwinding assay

The unwinding substrate was an RNA duplex composed of a 35-nucleotide strand and a 15-nucleotide strand (Fig. 3A). The 35-nucleotide RNA was generated by T7 RNA polymerase runoff transcription and purified by denaturing polyacrylamide gel electrophoresis (Lorsch and Herschlag 1998a). The DNA templates for the transcription were 5′-CCAGGAGGCTGTCGCTCTTAATGAC CTAGAGGTCCTATAGTGAGTCGTATTACATATGCGTGTTAC C-3′ and 5′-GGTAACACGCATATGTAATACGACTCACTATAGG-3′. The 15-nucleotide RNA was synthesized by using solid-phase methods and was obtained from the Stanford PAN Facility. The 15-nucleotide RNA was 5′-end-labeled with [γ-^{32}P]-ATP by using T4 polynucleotide kinase (NEB) and was purified on nondenaturing 20% polyacrylamide gel electrophoresis as described (Zaug et al. 1988; Herschlag et al. 1993).

Hybridized duplexes were prepared in annealing buffer (20 mM Tris-Cl at pH 7.4 and 80 mM potassium acetate) by heating the RNAs for 3 to 4 min at 90°C followed by cooling at room temperature for 10 min. Annealed duplex RNA was separated from ssRNA by using a 15% nondenaturing polyacrylamide gel (0.1 M Tris, 0.1 M boric acid, and 10 mM EDTA) with the running temperature maintained at 15°C. The band containing duplex was excised from the gel, soaked in annealing buffer at 4°C overnight, and stored at −20°C.

Reaction conditions and procedures

Unwinding assays were carried out at 25°C in the same buffer conditions as hydrolysis assays (25 mM MES-KOH, 12 mM Tris-Cl, 2.5 mM $MgCl_2$, 2.2 mM dithiothreitol, 6% glycerol, 60 μM EDTA, 34 mM potassium acetate, and 30 mM KCl at pH 6.0). Enzymes were diluted to desired concentrations with enzyme storage buffers. Reactions (typically 40 μL total volume) were performed with trace-labeled RNA duplex and were initiated by the addition of an excess of premixed eIF4B and eIF4A. Control reactions indicated that the unwinding rates are insensitive to the order of protein addition. Aliquots (5 μL) were removed from the reaction at five to eight specific times, mixed with 5 μL stop solution (2% SDS, 100 mM dithiothreitol, 10% glycerol, 0.1% bromphenol blue, and 50 mM Tris-Cl at pH 6.8) and immediately placed on ice. Stopped reactions were stable for several hours on ice without significant duplex reannealing or deannealing. Single-stranded product was separated from intact duplex by using 15% nondenaturing polyacrylamide gel electrophoresis (0.1 M Tris, 0.1 M boric acid, and 1 mM EDTA) at a constant temperature of 15°C. The fraction of ssRNA was quantified with a PhosphoImager (Molecular Dynamics).

Kinetic analysis

The fraction of ssRNA was plotted against time, and the data were fit to a first-order exponential by using KaleidaGraph (Synergy), yielding the observed first-order rate-constant $k_{obs,unw}$. Reactions typically reached completion with an endpoint of >85% product. The observed rate-constants for very slow reactions were determined from a linear fit of the first 10% of the reaction, assuming an endpoint of 90%. Duplex dissociation was slow ($k_{obs,unw} < 0.0001$ min^{-1}) in the absence of enzymes.

Apparent equilibrium binding constants ($K_{1/2}$) were determined by fitting the dependence of $k_{obs,unw}$ on the concentration of a reaction component to the Michaelis-Menten model (Segel 1993). Under these conditions, the $K_{½}$ for eIF4B (with ATP·Mg) is ~0.2 μM (data not shown).

Estimation of errors

Rate and thermodynamic constants obtained in independent experiments varied less than twofold. Reported errors represent the R values from the KaleidaGraph fits. Unless otherwise indicated,

reaction components were varied at least fivefold above and below K_M or $K_{1/2}$ values.

ACKNOWLEDGMENTS

Jon Lorsch and Matt Marshall performed initial unwinding experiments that greatly facilitated this work. Members of the Herschlag laboratory provided valuable advice and discussion. We thank James Berger, Jon Lorsch, Dave McKay, and members of the Herschlag laboratory for comments on the manuscript. This work was supported by a National Institutes of Health grant GM49243 to D.H.

The publication costs of this article were defrayed in part by payment of page charges. This article must therefore be hereby marked "advertisement" in accordance with 18 USC section 1734 solely to indicate this fact.

Received July 23, 2002; accepted July 24, 2003.

REFERENCES

Abramson, R.D., Dever, T.E., Lawson, T.G., Ray, B.K., Thach, R.E., and Merrick, W.C. 1987. The ATP-dependent interaction of eukaryotic initiation factors with mRNA. *J. Biol. Chem.* **262:** 3826–3832.

Abramson, R.D., Dever, T.E., and Merrick, W.C. 1988. Biochemical evidence supporting a mechanism for cap-dependent and internal initiation of eukaryotic mRNA. *J. Biol. Chem.* **263:** 6016–6019.

Benne, R. and Hershey, J.W.B. 1978. The mechanism of action of protein synthesis initiation factors from rabbit reticulocytes. *J. Biol. Chem.* **253:** 3078–3087.

Bi, X., Ren, J., and Goss, D.J. 2000. Wheat germ initiation factor eIF4B affects eIF4A and eIFiso-4F helicase activity by increasing the ATP binding affinity of eIF4A. *Biochemistry* **39:** 5758–5765.

Blum, S., Schmid, S.R., Pause, A., Buser, P., Linder, P., Sonenberg, N., and Trachsel, H. 1992. ATP hydrolysis by initiation factor 4A is required for translation initiation in *Saccharomyces cerevisiae*. *Proc. Natl. Acad. Sci.* **89:** 7664–7668.

Browning, K., Fletcher, L., Lax, S., and Ravel, J. 1989. Evidence that the 59-kDa protein synthesis initiation factor from wheat germ is functionally similar to the 80-kDa initiation factor 4B from mammalian cells. *J. Biol. Chem.* **264:** 8491–8494.

Caruthers, J.M. and McKay, D.B. 2002. Helicase structure and mechanism. *Curr. Opin. Struct. Biol.* **12:** 123–133.

Catrina, I.E. and Hengge, A.C. 1999. Comparisons of phosphorothioate and phosphate monoester transfer reactions: Activation parameters, solvent effects, and the effect of metal ions. *J. Am. Chem. Soc.* **121:** 2156–2163.

Cohn, M. 1982. Some properties of the phosphorothioate analogues of adenosine triphosphate as substrates of enzymic reactions. *Acc. Chem. Res.* **15:** 326–332.

Domanico, P., Mizrahi, V., and Benkovic, S.J. 1986. Observations on the chemistry of phosphorothioate transfer. In: *Mechanisms of enzymatic reactions: Stereochemistry*, pp. 127–138. Elsevier, Amsterdam, The Netherlands.

Eckstein, F. 1983. Phosphorothioate analogues of nucleotides: Tools for the investigation of biochemical processes. *Angew Chem. Int. Ed. Engl.* **22:** 423–439.

———. 1985. Nucleoside phosphorothioates. *Ann. Rev. Biochem.* **54:** 367–402.

Frey, P.A. and Sammons, R.D. 1985. Bond order and charge localization in nucleoside phosphorothioates. *Science* **228:** 541–545.

Gorbalenya, A.E. and Koonin, E.V. 1993. Helicases: Amino acid sequences comparisons and structure-function relationships. *Curr. Opin. Struct. Biol.* **3:** 419–429.

Grifo, J.A., Abramson, R.D., Satler, C.A., and Merrick, W.C. 1984. RNA-stimulated ATPase activity of eukaryotic initiation factors. *J. Biol. Chem.* **259:** 8648–8654.

Herschlag, D., Eckstein, F., and Cech, T.R. 1993. Contribution of 2′-hydroxyl groups of the RNA substrate to binding and catalysis by the *Tetrahymena* ribozyme: An energetic picture of an active-site composed of RNA. *Biochemistry* **32:** 8299–8311.

Hollfelder, F. and Herschlag, D. 1995. The nature of the transition state for enzyme-catalyzed phosphoryl transfer: Hydrolysis of O-aryl phosphorothioates by alkaline phosphatase. *Biochemistry* **34:** 12255–12264

Korolev, S., Yao, N., Lohman, T.M., Weber, P.C., and Waksman, G. 1998. Comparisons between the structures of HCV and Rep helicases reveal structural similarities between SF1 and SF2 superfamilies of helicases. *Protein Sci.* **7:** 605–610.

Kozak, M. 1986. Influences of messenger-RNA secondary structure on initiation by eukaryotic ribosomes. *Proc. Natl. Acad. Sci.* **83:** 2850–2854.

———. 1992. A consideration of alternative models for the initiation of translation in eukaryotes. *Crit. Rev. Biochem. Mol. Biol.* **27:** 385–402.

Linder, P. and Slonimski, P.P. 1989. An essential yeast protein, encoded by duplicated genes TIF1 and TIF2 and homologous to the mammalian translation initiation factor eIF4A, can suppress a mitochondrial missense mutation. *Proc. Natl. Acad. Sci.* **86:** 2286–2290.

Lorsch, J.R. and Herschlag, D. 1998a. The DEAD box protein eIF4A, 1: A minimal kinetic and thermodynamic framework reveals coupled binding of RNA and nucleotide. *Biochemistry* **37:** 2180–2193.

———. 1998b. The DEAD box protein eIF4A, 2: A cycle of nucleotide and RNA-dependent conformational changes. *Biochemistry* **37:** 2194–2206.

Matson, S.W. and George, J.W. 1987. DNA helicase II of *Escherichia coli*. *J. Biol. Chem.* **262:** 2066–2076.

Merrick, W.C. and Hershey, J.W.B. 1996. The pathway and mechanism of eukaryotic protein synthesis. In: *Translational control* (eds. J. Hershey et al.), pp. 31–70. Cold Spring Harbor Laboratory Press, Cold Spring Harbor, NY.

Pause, A., Methot, N., and Sonenberg, N. 1993. The HRIGRXXR region of the DEAD box RNA helicase eukaryotic translation initiation factor 4A is required for RNA binding and ATP hydrolysis. *Mol. Cell. Biol.* **13:** 6789–6798.

Peck, M.L. and Herschlag, D. 1999. Effects of oligonucleotide length and atomic composition on stimulation of the ATPase activity of translation initiation factor eIF4A. *RNA* **5:** 1210–1221.

Pecoraro, V.L., Hermes, J.D., and Cleland, W.W. 1984. Stability constants of Mg^{2+} and Cd^{2+} complexes of adenosine nucleotides and thionucleotides and rate constants for the formation and dissociation of MgATP and MgADP. *Biochemistry* **23:** 5262–5271.

Pelletier, J. and Sonenberg, N. 1985. Insertion mutagenesis to increase secondary structure within the 5′ noncoding region of a eukaryotic messenger-RNA reduces translational efficiency. *Cell* **40:** 515–526.

Richter-Cook, N.J., Dever, T.E., Hensold, J.O., and Merrick, W.C. 1998. Purification and characterization of a new eukaryotic protein translation factor. *J. Biol. Chem.* **273:** 7579–7587.

Rogers Jr., G.W., Richter, N.J., and Merrick, W.C. 1999. Biochemical and kinetic characterization of the RNA helicase activity of eukaryotic initiation factor 4A. *J. Biol. Chem.* **274:** 12236–12244.

Rogers Jr., G.W., Lima, W.F., and Merrick, W.C. 2001a. Further characterization of the helicase activity of eIF4A: Substrate specificity. *J. Biol. Chem.* **276:** 12598–12608.

Rogers Jr., G.W., Richter, N.J., Lima, W.F., and Merrick, W.C. 2001b. Modulation of the helicase activity of eIF4A by eIF4B, eIF4H, and eIF4F. *J. Biol. Chem.* **276:** 30914–30922.

Rozen, F., Edery, I., Meerovitch, K., Dever, T.E., Merrick, W.C., and Sonenberg, N. 1990. Bidirectional RNA helicase activity of eucaryotic translation initiation factors 4A and 4F. *Mol. Cell. Biol.* **10:** 1134–1144.

Segel, I.H. 1993. *Enzyme kinetics: Behavior and analysis of rapid equi-*

librium and steady-state enzyme systems. John Wiley and Sons, New York.

Singleton, M.R. and Wigley, D.B. 2002. Modularity and specialization in superfamily 1 and 2 helicases. *J. Bacteriol.* **184:** 1819–1826.

Smith, C.A. and Rayment, I. 1996. Active site comparisons highlight structural similarities between myosin and other P-Loop proteins. *Biophys. J.* **70:** 1590–1602.

Staley, J.P. and Guthrie, C. 1998. Mechanical devices of the spliceosome: Motors, clocks, springs, and things. *Cell* **92:** 315–326.

Stole, E. and Bryant, F.R. 1997. The rate-determining step on the recA protein–catalyzed ssDNA-dependent ATP hydrolysis reaction pathway. *Biochemistry* **36:** 3483–3490.

Svitkin, Y.V., Pause, A., Haghighat, A., Pyronnet, S., Witherell, G., Belsham, G.J., and Sonenberg, N. 2001. The requirement for eukaryotic initiation factor 4A (eIF4A) in translation is in direct proportion to the degree of mRNA 5′ secondary structure. *RNA* **7:** 382–394.

Tanner, N.K. and Linder, P. 2001. DExD/H box RNA helicases: From generic motors to specific dissociation functions. *Mol. Cell* **8:** 251–262.

Trachsel, H., Erni, B., Schreier, M.H., and Staehelin, T. 1977. Initiation of mammalian protein-synthesis, 2: Assembly of initiation complex with purified initiation-factors. *J. Mol. Biol.* **116:** 755–767.

Vale, R.D. and Milligan, R.A. 2000. The way things move: Looking under the hood of molecular motor proteins. *Science* **288:** 88–95.

Velankar, S.S., Soultanas, P., Dillingham, M.S., Subramanya, H.S., and Wigley, D.B. 1999. Crystal structures of complexes of PcrA DNA helicase with a DNA substrate indicate an inchworm mechanism. *Cell* **97:** 75–84.

Wagner, J.D.O., Jankowsky, E., Company, M., Pyle, A.M., and Abelson, J.N. 1998. The DEAH-box protein Prp22 is an ATPase that mediates ATP-dependent mRNA release from the spliceosome and unwinds RNA duplexes. *EMBO J.* **17:** 2926–2937.

Wong, I. and Lohman, T.M. 1992. Allosteric effects of nucleotide cofactors on *Eschericia coli* Rep helicase-DNA binding. *Science* **256:** 350–355.

Zaug, A.J., Grosshan,s C.A., and Cech, TR. 1988. Sequence-specific endoribonuclease activity of the *Tetrahymena* ribozyme: Enhanced cleavage of certain oligonucleotide substrates that form mismatched ribozyme substrate complexes. *Biochemistry* **27:** 8924–8931.

Zhang, Y.-L., Hollfelder, F., Gordon, S.J., Chen, L., Keng, Y.-F., Wu, L., Herschlag, D., and Zhang, Z.-Y. 1999. Impaired transition state complementarity in the hydrolysis of O-arylphosphorothioates by protein-tyrosine phosphotases. *Biochemistry* **38:** 12111–12123.

Adenosine 5′-O-(3-thio)triphosphate (ATPγS) is a substrate for the nucleotide hydrolysis and RNA unwinding activities of eukaryotic translation initiation factor eIF4A

MATTHEW L. PECK and DANIEL HERSCHLAG

RNA 2003 9: 1180-1187